CHAPTER C.8
WETLAND NOURISHMENT MODULE

Jenneke M. Visser[1] (Chair)
John Callaway[2]
Denise Reed[3]
Gregory D. Steyer[4]
Joe Suhayda[5]
Erick Swenson[1]

[1] *Coastal Ecology Institute, Louisiana State University, Baton Rouge.*
[2] *Department of Environmental Science, University of San Francisco, San Francisco.*
[3] *Department of Geology and Geophysics, University of New Orleans, New Orleans*
[4] *U.S. Geological Survey, National Wetlands Research Center, Baton Rouge*
[5] *Center for GeoInformatics, Louisiana State University, Baton Rouge*

8.1   Introduction

The objective of this module is to predict the effects of different restoration scenarios on the amount of wetland area along the coast for 50 years into the future. This module uses a combination of empirical relationships and landscape analogs to reflect the complex processes controlling land change in the Louisiana coastal zone. The original intent for this module was to predict elevation changes that than could be used by the habitat switching module to predict habitat changes, which included the change from water to different wetland habitats. While it was not possible, within the limits of available data, to assess elevation changes per se, elevation is indirectly reflected by changes in the land-water configuration.

8.2   Rationale of Assumptions

8.2.1   Elevation Component

Several existing models for elevation prediction in coastal wetlands exist (*e.g.* Morris and Bowden 1986, Chmura *et al.* 1992, Callaway *et al* 1996, Rybczyk and Cahoon 2002). These models all follow a similar conceptual model (Figure C.8-1), but the application of these models in the current LCA setting would require many assumptions and/or unavailable data sets when used coastwide (*e.g.* compaction, bulk density profiles). It was therefore decided to explore the use of existing measurements of long-term accretion using the 1963 peak of ^{137}Cs as a marker (see Pennington *et al.* 1973) to encompass surface accumulation and soil compaction processes over decades rather than attempting the explicit process-based approach used in many of the models. Conceptually the use of long-term accretion measurements using ^{137}Cs or ^{210}Pb is similar to the model approach (Figure C.8-1), since the long-term measurements integrate all of the processes in the conceptual model except for deep subsidence. These ^{137}Cs accretion measurements have been taken throughout the Louisiana coastal zone (see Figure C.8-2) and an effort was made to relate accretion rates to such factors as distance from the sediment source (*e.g.* coastal bays or source of riverine sediments),

habitat type, organic matter content of the soil, and/or soil type. However we found that accretion was not significantly correlated with any of these factors except that accretion cores under the influence of a major distributary of the Mississippi River *(i.e.* Mississippi River Delta, Atchafalaya Bay, Wax Lake Outlet) showed substantially higher accretion (Figure C.8-3).
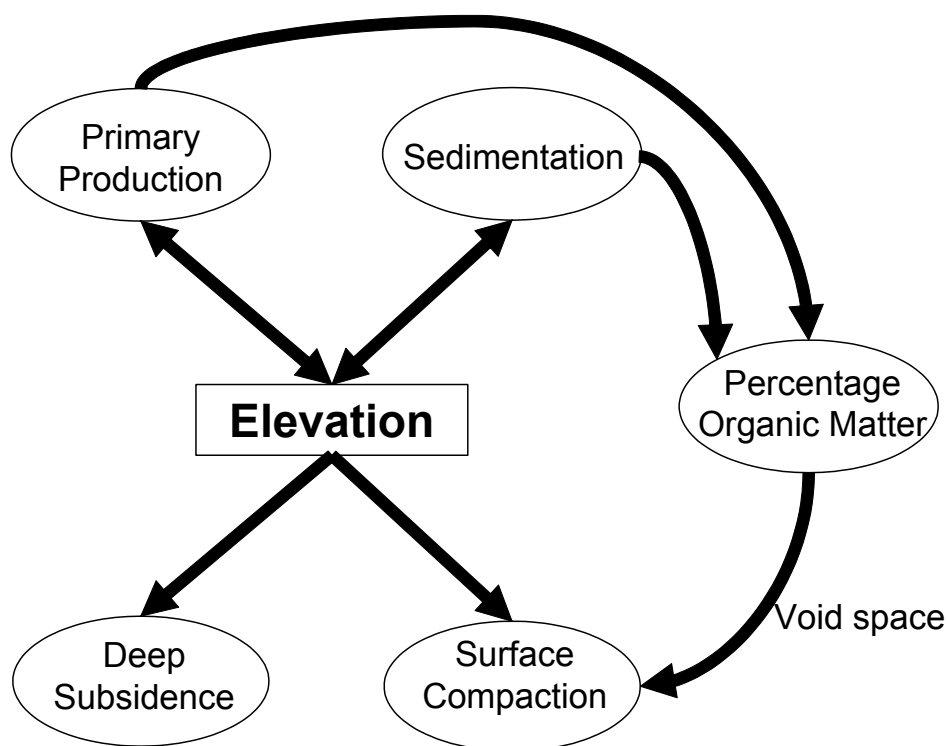
Conceptual Elevation Model

Figure C.8-1 Conceptual Model of Elevation Change Used in Existing Soil Formation Simulation Models
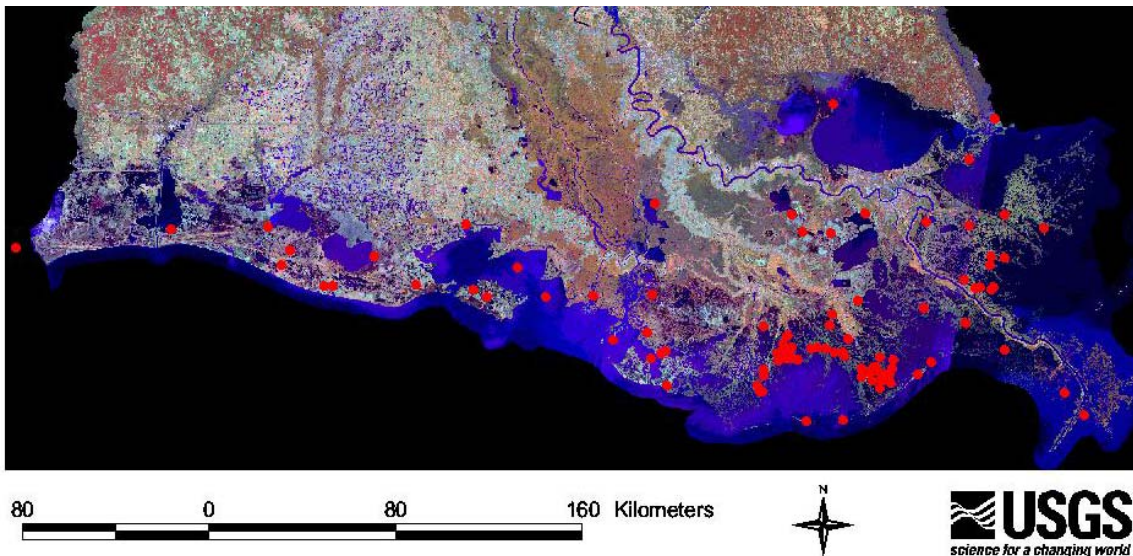
Figure C.8-2   Distribution of existing Cesium core data analyzed for this module.
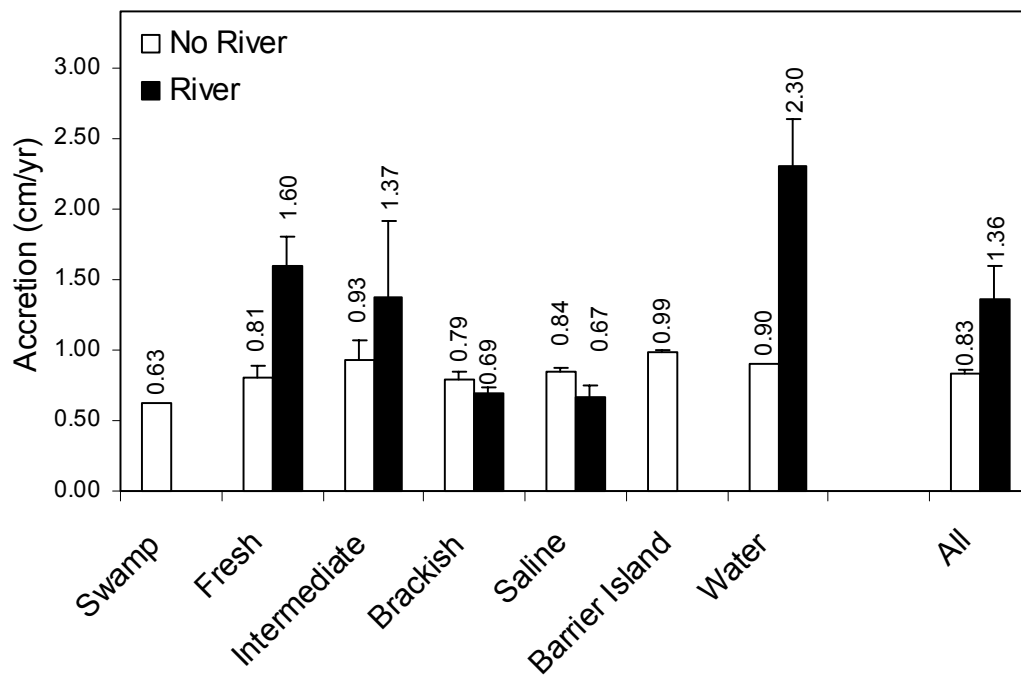

Figure C.8-3   Accretion rates by habitat and river influence. Error bars reflect one standard error. River influenced rates are based on four or fewer cores per marsh type.

In addition, the measured background accretion rates were assessed in relation to subsidence and sea-level rise data. Long-term (*i.e.*, Holocene) subsidence rates have been determined using ^{14}C dating of buried marsh peats and Gagliano (1999) present such data for the Louisiana coast. However, using the depth of the buried horizon to represent subsidence alone is misleading as during the period since peat deposition sea-level has also risen. Kulp (2000) has compared Holocene sea-level rise curves to the ^{14}C data from cores, allowing the subsidence component to be isolated (Figure C.8-4). These long-term subsidence rates represent the average subsidence over thousands of years (the exact period varies among dated deposits and cores). The accretion rates shown in the recent cores (Figure C.8-3) are high enough to keep pace with these long-term rates. Recent rates of subsidence, as reflected in tide gauge measurements (Penland and Ransey 1991) indicate higher rates of subsidence in the 20th century and although the reasons for the difference between long and short-term rates is not yet clear, Morton *et a.l* (2002) has identified localized areas of high subsidence associated with hydrocarbon withdrawals from onshore reservoirs. The accretion data (based on accumulation of soil since 1963) encompass the period when tide gauge records show high subsidence and when Morton *et al.* suggest that faults may have been reactivated by oil and gas extraction activities. These recent insights into subsidence processes in the Louisiana coastal zone, showing large differences between long-term rates and near-past rates of subsidence, and the association of high subsidence with human activities which are now substantially reduced, make the projection of subsidence into the future problematic. In addition, accretion cores are generally taken in the marsh that survived during a period of high subsidence and therefore these accretion rates reflect those areas that by definition have kept up with relative sea level rise.
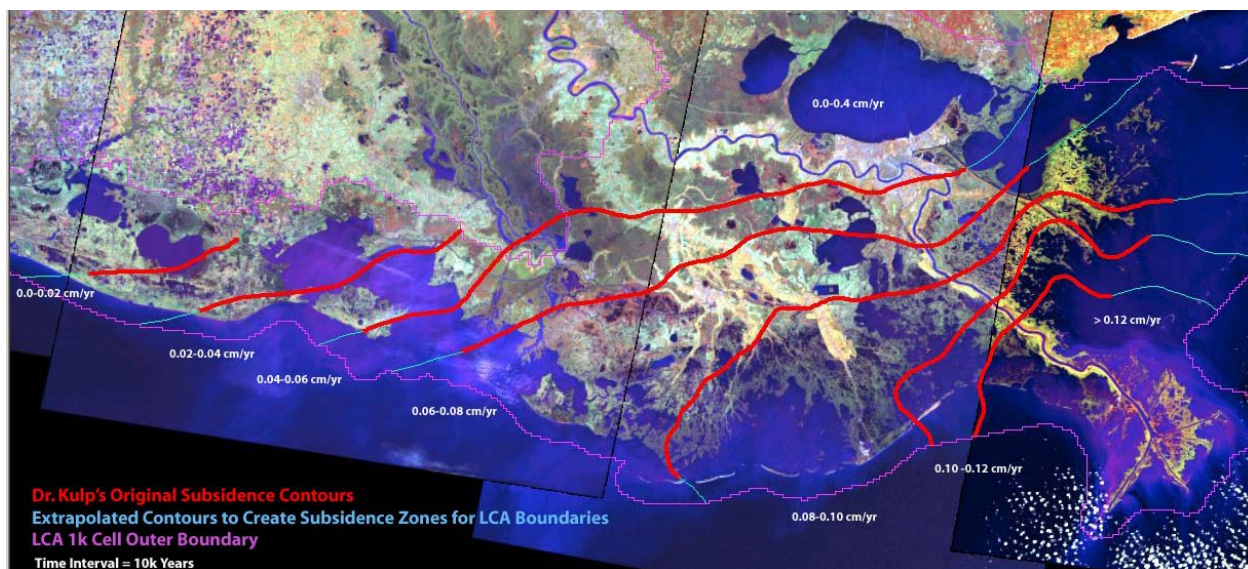

Figure C.8-4   Subsidence rates for the Louisiana coastal area (based on Kulp 2000).

Consequently, it is not possible to explicitly project relative elevation into the future due to uncertainties regarding future subsidence rates and the limited availability of accretion data. Therefore, this module was limited to the prediction of land change.

8.2.2 Land-Change Component

Historic land change rates were provided by Barras *et al.* (2003). This group analyzed historic land change patterns and identified polygons of similar land loss. Data were provided with land-loss assigned to several categories (Table C.8-1) and reflect the change from 1978 to 1990. The land loss rates provided did not include the future projection changes made by Barras *et al* (2003) based on approved CWPPRA and WRDA projects.

Table C.8-1   Land loss rate categories based on land area changes between 1978 and 1990

Land Loss Rate Categories (%/yr)	
0	-0.0060
-0.0015	-0.0075
-0.0030	-0.0090
-0.0045	-0.0120
-0.0050	-0.0150

8.2.3 Land building

The land building module (Suhayda *et al.* 2003) predicts land formation in the direct impact area of the different diversion areas. It is possible to make a more spatially explicit projection of land building associated with riverine inputs if the current areas of influence are overlaid on the .3 mi^2 (1 km^2) grid and this will allow estimation of changes, at the .3 mi^2 (1 km^2) scale, of changes in land-water ratio. This application of the land building module requires that the water within each cell be categorized as either ponds (GIS category marsh water), open water (GIS category water water), and channels (recognizing that in natural deltaic systems, land areas are not solid and channels are present). The volume to be filled will be based on the area of existing marsh ponds times a depth of 1.64 ft (50 cm) (assumed average based on team field experience) and the area of open water minus the water that will remain as channel times the depth. Based on the 1990 configuration of the Wax Lake Delta, an average .3 mi^2 (1 km^2) area has 35% open water in channels; these channels have an average depth of 5 ft (van Heerden 1983). Therefore, the remaining channel water volume in a cell after ponds and open water are filled is 18,836,783 cubic feet. The fill rate will be calculated using the algorithm in the current land building module. Filling will start in the cell with available area to fill closest to the diversion input and will spread to adjacent cells based on proximity to the diversion point and availability of fill area (Figure C.8-5).
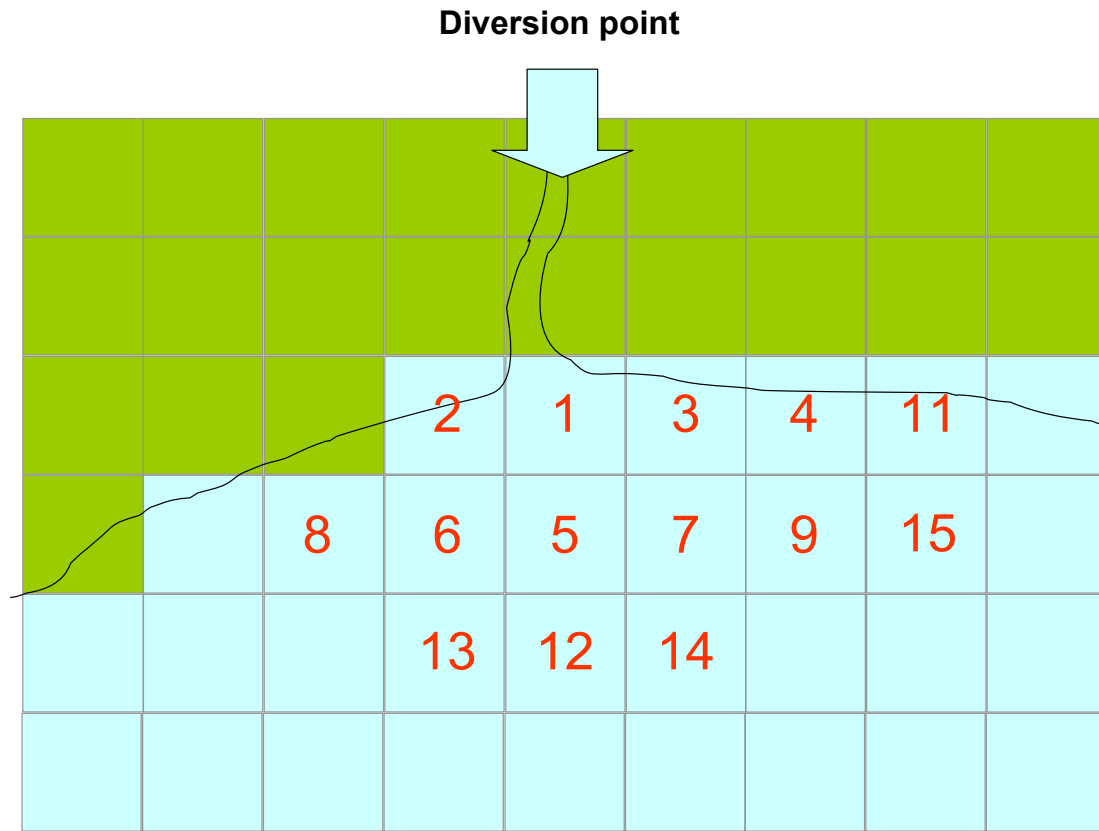
Diversion point

Figure C.8-5 Generalized order at which cells will be filled with sediments from the diversion. This order is determined based on the distance of the cell from the diversion.

8.2.4   Nourishment Component

All cells will follow historic land loss rates for the area (see Barras *et al.* 2003 and discussion above) unless affected by land building or nourishment effects. The nourishment effect of reintroduction of river water is based on the effects of the Atchafalaya River in nourishing marshes of western Terrebonne Basin in the late 20th century. This effect was derived using a relationship between land change rate (in a 1 km^2 cell) and the distance from the mouth of the Atchafalaya River (Figure C.8-6, 8-7). The land change rate was calculated as follows:

Land Change Rate = (%LAND1-%LAND0) / (TIME1-TIME0)

Where %LAND0 = the percentage of the area the area at the beginning of the period, %LAND1 = the percentage of the area the area at the end of the period, TIME0 = the time of the first land area estimate in decimal years, and TIME1 = the time of the second land estimate in decimal years.

LCA - 1956 - 1990 Percent Land Change
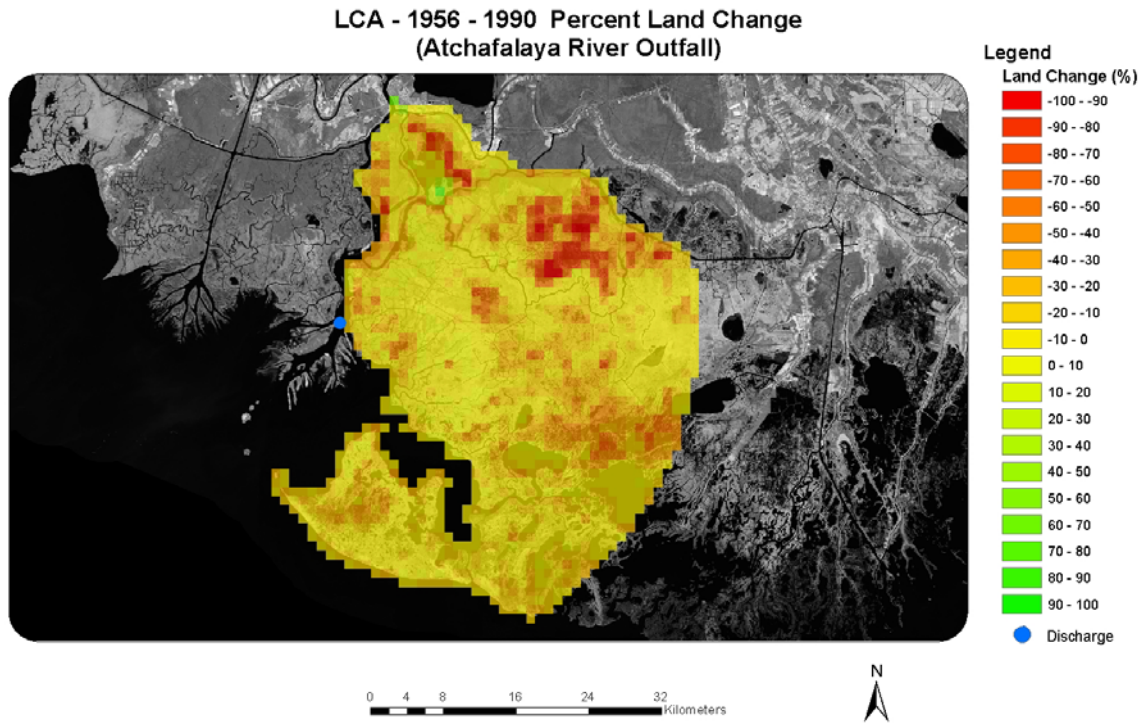(Atchafalaya River Outfall)

Figure C.8-6 Land change pattern away from the mouth of the Atchafalaya Delta. Only the east side of the mouth was used, because of the effect of the Wax Lake Delta to the west.
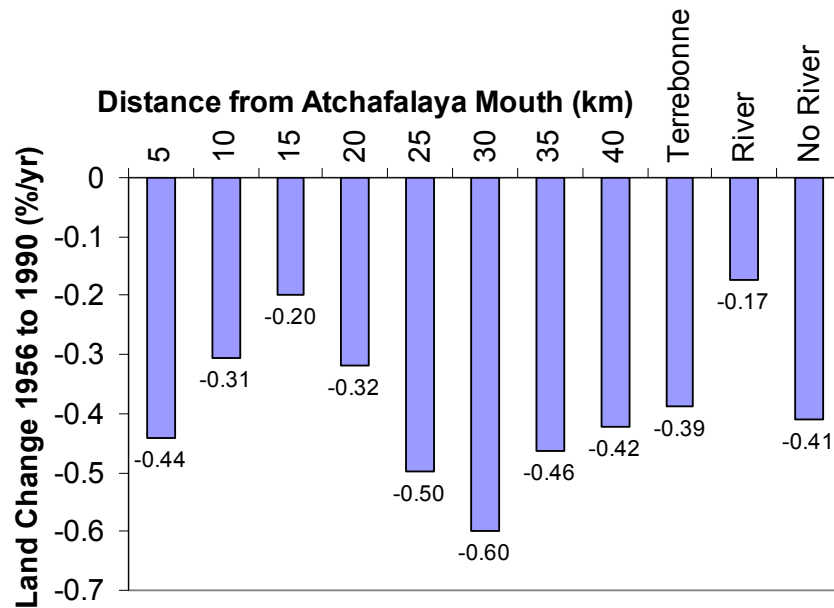

Figure C.8-7   Pattern of land change (% of the total area per year)

An examination of land change rates with distance from the river mouth or diversion point in 3 mi (5 km) increments showed that land loss is reduced in the area between 3 and 12 mi (5 and 20 km) away from the river, with the greatest reduction in the area 6 and 9 mi (6.2 mi (10 km) to 9.3 mi (15 km)) away from the diversion point (Figure C.8-7 and 8-8). This is the nourishment effect and reflects the increased accretion rates in river influenced areas (see Figure C.8-3). The lack of reduction of land loss within the 3 mi (5 km) range of the river mouth is most likely due to erosion along channels (Letter 1982; van Heerden 1983). Since the Atchafalaya is one of the larger diversions of Mississippi River Water and at the high end of the range of alternatives reviewed with this module, we reviewed recent land loss changes at Caernarvon (USGS unpublished data) a diversion that started operations in 1991 and has an average discharge of 1,271 cfs to determine any differences due to discharge size. This analysis showed the same general relationship as the Atchafalaya analysis (Figure C.8-8 and 8-9).
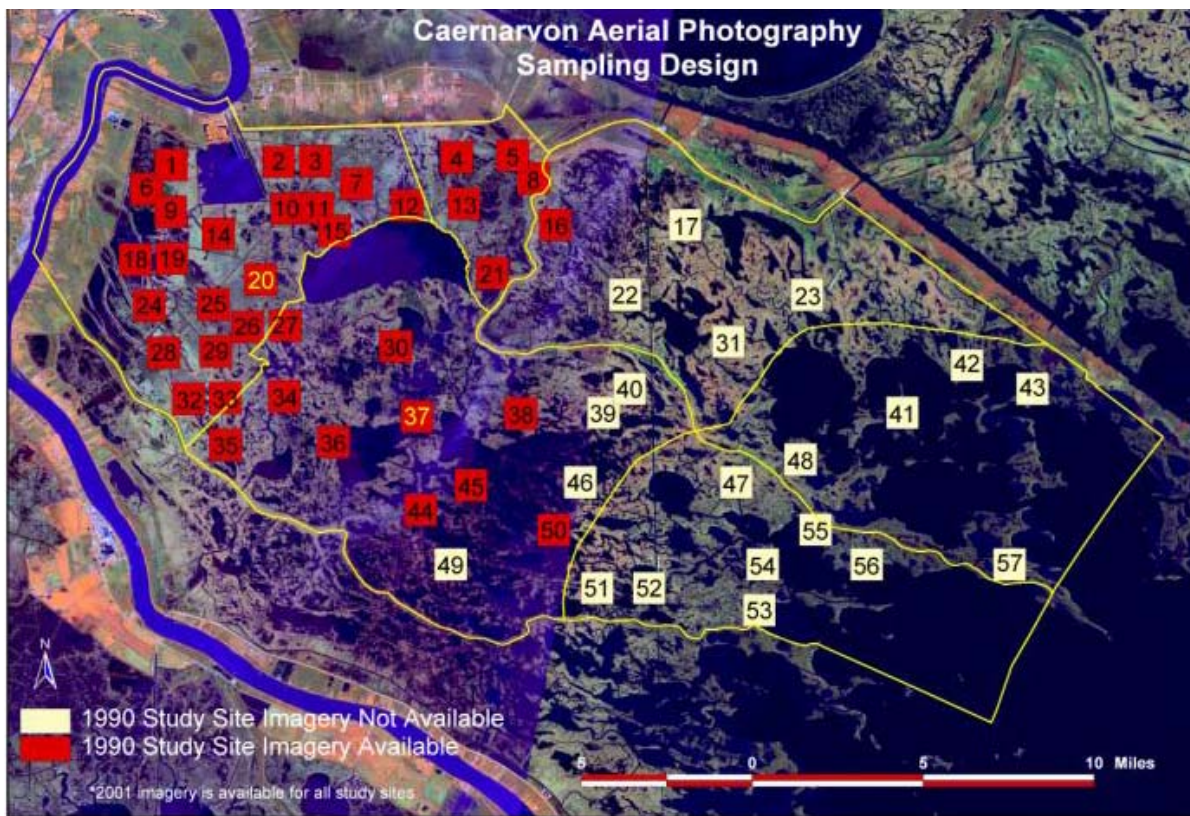

Figure C.8-8 Distribution of Study Sites Used to Test Effect of Caernarvon Diversion on Land Change Rates
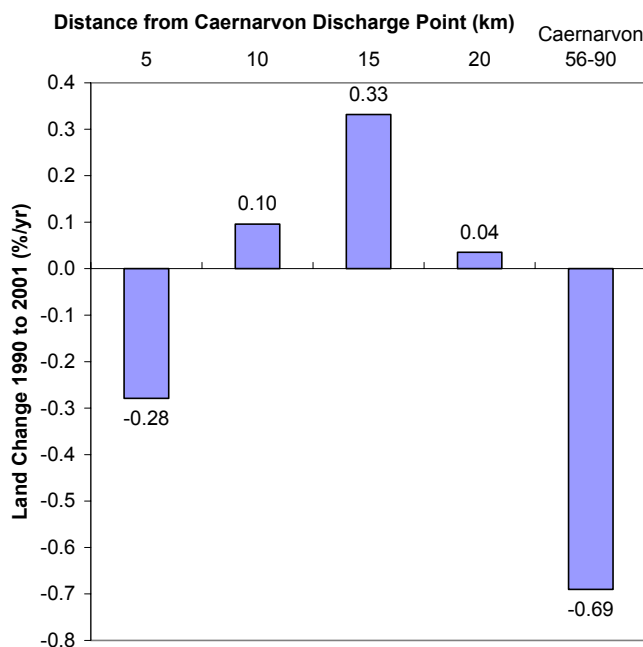
Figure C.8-9   Pattern of Land Change

8.2.5   Spatial and Temporal Scales

This module will use a 1 km^2 cell size and a decadal time step.

8.3   Desktop Algorithms

8.3.1   Land Building

The volume available for land building in cubic yards per year is determined with the following formula:

Sediment Volume= Annual Sediment Load / Bulk Density of Deposited Sediment

The annual sediment load for each diversion is given in tons per year. This weight of sediment is transformed to volume based on the bulk density of deltaic soils in grams per cubic centimeter (which is the same as tons per cubic yard). However, not all of the sediment is retained. A large percentage remains in suspension and is transported to the Gulf of Mexico. We determined this retention coefficient based on the information for the Wax Lake Delta.

The Wax Lake Outlet channel was constructed in 1942 (Roberts *et al.* 1980). However, prior to the mid 1950's, most of the sediment was trapped in the Atchafalaya Basin (Cratsley 1975). Data on the average daily sediment load of the Atchafalaya River at Simmesport from October 1972 through September 1989 were obtained from the USGS database (http://webserver.cr.usgs.gov/ sediment/ seddatabase.cfm). The average sediment load of the Atchafalaya River at Simmesport is 254,444 ton per day or 92,871,932 ton per year. It was assumed that 10% of this load was captured in the Atchafalaya Basin (period 1955 through 1990); therefore the remaining load is 83,584,739 tons per year. It was also

assumed that the proportion of the sediment load is equivalent to the proportion of discharge. Wax Lake receives 40 % of the Atchafalaya Discharge (Letter 1982); therefore the sediment load delivered to the Wax Lake Outlet is 25,075,422 tons per year. The bulk density of deltaic soils is 0.835 gram per cubic centimeter (Faulkner and Poach 1996). Thus the Wax Lake area receives enough sediment to fill 30,030,445 cubic yards per year. If all this sediment was retained and assuming that the Atchafalaya Bay was 6 feet deep and 35 years of delivery (1955 to 1990) this would build 439 square kilometers. However, there were only 30 km^2 of land present in the delta in 1990 (R. Cunningham personal communication) in addition to the infilling of Wax Lake. Therefore, assuming that 15% of the sediment load is retained in the area gives the reasonable answer of 66 kilometer square of area created, given our assumptions regarding water depth and discharge-sediment load relationships. This 15 percent retention rate is in the same range as the 17 percent average 50-year retention rate determined with a HAD-1 simulation model (Thomas *et al.* 1982). The HAD-1 simulation model slightly over-estimated sub-aerial delta growth. This retention is the long term retention of sediments and includes sediments needed to keep up with local subsidence and sea level rise.

8.3.2   Nourishment

Both diversions (Atchafalaya and Caernarvon) showed a similar pattern of maintained land-loss within 3.1 mi (5 km) from the diversion point (probably because of scouring of channels) with reduction in loss (or even gain) in the areas between 3.1 mi (5 km) and 12.4 mi (20 km) from the diversion point. The maximum positive effect seems to occur 6.2 mi (10 km) to 9.3 mi (15 km) from the diversion point (see Figure C.8-7 and 8-9). However, there is a difference in the magnitude of change, with gains observed in the Caernarvon area with a relatively small discharge of 1,271 cfs, while continued, though reduced, loss in the Atchafalaya area with 177,135 cfs. This is probably partially due to the higher background loss rate in the Atchafalaya area (Figure C.8-7).

Another difference is that the marshes in the 12.4 mi (20 km) range of the Atchafalaya were fresh in 1968 (Chabreck 1972), while the brackish marsh at Caernarvon has changed to intermediate marsh from 1990 to 2001 (Linscombe *et al.* 2001). Accretion data (Figure C.8-3) indicate significantly higher accretion in fresh and intermediate marshes influenced by rivers, while accretion seems unaffected by river input in brackish and saline marshes with river influence. In the Atchafalaya area it is relatively straightforward to distinguish direct land building from the nourishment component, while at Caernarvon these two effects occur simultaneously. This probably partially explains the higher reduction in land loss around the Caernarvon diversion.

Therefore the nourishment algorithm subtracts 0.21%/year (see Table C.8-2) from the loss rates for cells that are within 6.2 mi (10 km) to 9.3 mi (15 km) from a diversion point, and reduces the loss rates of cells within the 3.1 mi (5 km) to 6.2 mi (10 km) range and the 9.2 mi (15 km) to 12.4 mi (20 km) range by 0.10 percent/year for those cells that were dominated by fresh marsh at year 0 (based on data from the Atchafalaya region; see Table C.8-1). For cells that were not fresh marsh in year 0 and are within the 6.2 mi (10 km) to 9.3 mi (15 km) range the loss rate will be reduced by 1.02 percent/year and cells in the 3.1 mi (5 km) to 6.2 mi (10 km) range and 9.2 mi (15 km) to 12.4 mi (20 km) range the loss rate will be reduced by 0.76 percent/yr (see Table 2).

The algorithm applies the land building algorithm first, cells that receive land building are not affected by land change rates (historic and/or nourishment). Cells unaffected by landbuilding are affected by the land change rate, but can not increase wetland area beyond the available area (cell area minus upland area).

Table C.8-2   Change in Percentage Land Area Per Year with Distance From the Diversion Point

	Atchafalaya (fresh marshes)		Caernarvon (brackish marshes)	
	Loss Rate (%/year)	Number of Observations	Loss Rate (%/year)	Number of Observations
Background	-0.41		-0.69	
5 to 10 km	-0.31	85	0.10	13
10 to 15 km	-0.20	159	0.33	13
15 to 20 km	-0.32	258	0.04	5
Absolute Difference				
5 to 10 km	0.10	85	0.79	13
10 to 15 km	0.21	159	1.02	13
15 to 20 km	0.09	258	0.73	5

8.3.3   Salinity Reduction Effect

In subprovince 4, the major effect on land change is not through diversions, but through hydrologic modifications that reduce the salinity stress on the vegetation. To our knowledge, no data are currently available that relate salinity reduction with reduction in land loss. We used the relative reduction in land loss in brackish marshes versus fresh marshes (Table C.8-2) to estimate this reduction. It was estimated that the Caernarvon diversion reduces salinity in the 9.2 mi (15 km) to 12.4 mi (20 km) range by 5 ppt. This reduction is reflected by a 0.64 % (0.73 minus 0.09) reduction in land loss. At 0 reduction in salinity the reduction in land loss should be 0. Based on these two points, we used the following formula to relate salinity reduction to land loss:

$$\text{Land Loss Reduction} = 0.128 * \text{Salinity Reduction}$$

It was assumed that no land gain results from salinity reduction. Therefore the resulting land change rate (historic land loss plus loss reduction) was restricted so that it could not exceed 0.

8.3.4   Marsh Creation

Several of the proposed measures included marsh creation and/or barrier island restoration. The created areas and timing of creations were obtained from the LCA co-location team. These areas were added in the year of creation and the cells land change rates (historic and nourishment) were applied to them.

8.4   Results

The land change module was used to predict the amount of land at year 50 under all different restoration alternatives within each subprovince. To illustrate these results we are using subprovince 1 results as an example, but results from the other subprovinces are comparable. As expected, increased sediment loads result in increased land area in year 50 (Figure C.8-9).
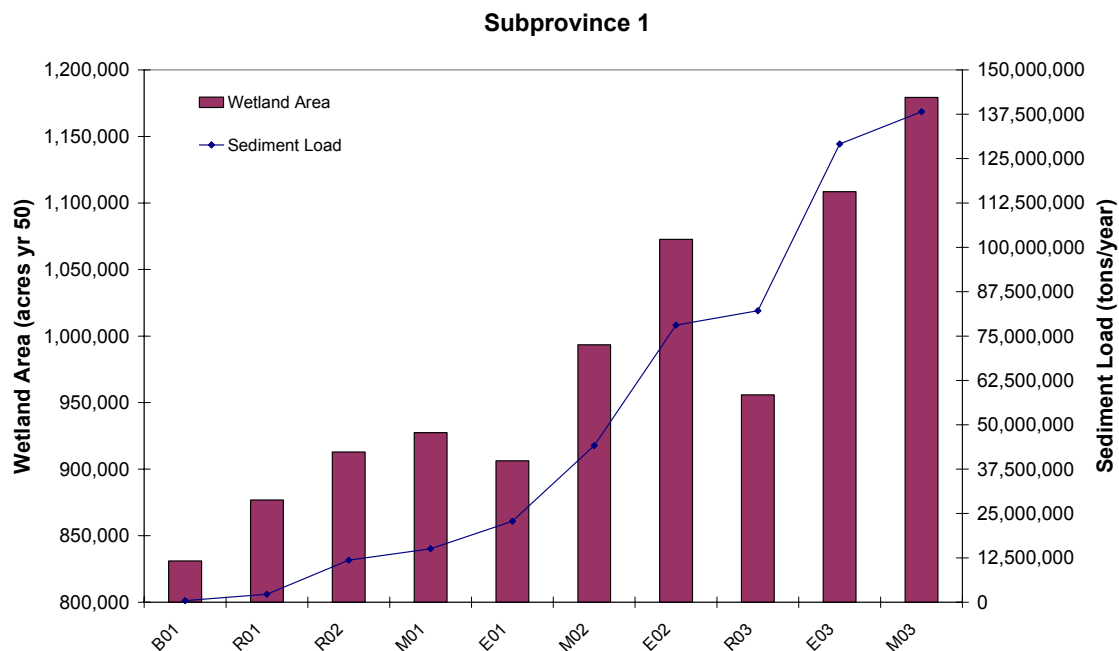

Subprovince 1

Figure C.8-9   Wetland area in Year 50 as a Result of Different Restoration Scenarios in Order of Increased Sediment Load

The model results can also be represented spatially (Figure C.8-10).   Figure C.8-10 shows year 50 under no action versus restoration scenario M02. The land building associated with the large diversion (110,000 cfs) into American/California Bay are easily recognized in Figure C.8-10, while other diversion locations are harder to spot at this scale.
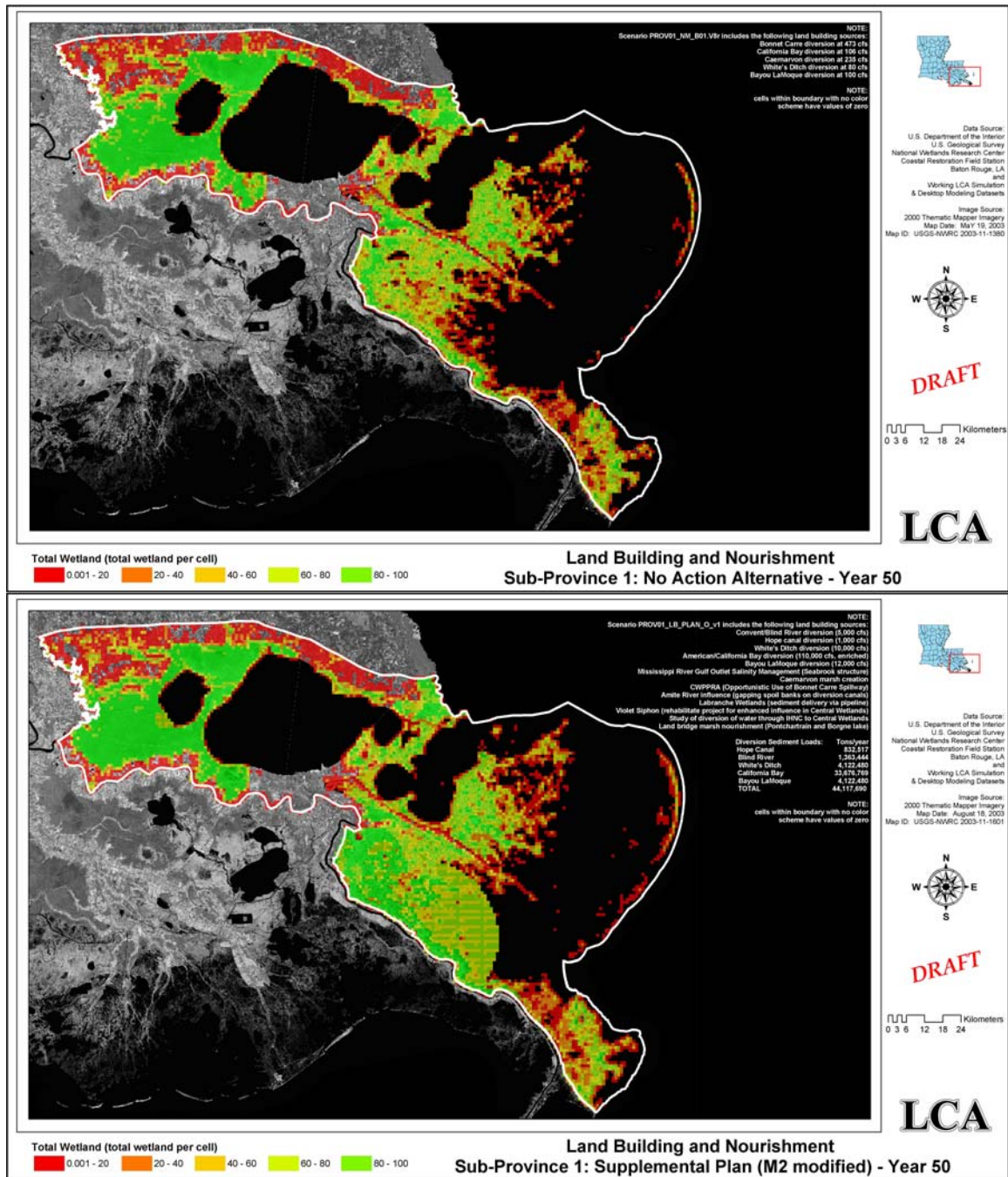
Figure C.8-10 Example of the Spatial Representation of Results from the Land Change Module